7 Renal Cell Carcinoma

David W. Barker and Ronald J. Zagoria

CONTENTS

7.1 Introduction

With a variety of imaging modalities in his or her armamentarium, the genitourinary radiologist plays an important role in the detection and management of patients with renal cell carcinoma (RCC). Appropriate and cost-effective use of these modalities, proper recognition of specific benign and malignant radiological features, and the keenness to "pick up" the sometimes subtle finding of an incidental renal mass on a study ordered for another purpose are all required skills.

D. W. Barker, MD
Senior Radiologist, Tennessee Cancer Specialists, PLLC, Medical Director, LifeCare Partners, LLC, 1450 Dowell Springs Boulevard, Suite 230, Knoxville, TN 37909, USA
R. J. Zagoria, MD, FACR
Professor of Radiology, Section Head of Abdominal Imaging, Vice-Chairman for Clinical Affairs, Department of Radiology, Wake Forest University School of Medicine, Medical Center Boulevard, Winston-Salem, NC 27157, USA

7.2 General Discussion

7.2.1 Incidence

Renal cell carcinoma, also known as renal adenocarcinoma, Grawitz tumor, hypernephroma, and renal clear cell carcinoma, is the most common neoplasm of the kidney, accounting for 90–95% of all renal tumors (Landis et al. 1999). The incidence of RCC has been rising steadily over the past 50 years (Chow et al. 1999), and approximately 30,000 new cases are now diagnosed in the United States annually (American Cancer Society 1996). Renal cell carcinoma accounts for 3% of all adult malignancies, and it is the sixth leading cause of cancer death (Greenlee et al. 2000).

7.2.2 Histology

Renal cell carcinoma arises from renal tubular epithelium and usually develops in the cortex of the kidney. Based on morphological and molecular characterization, there are four subtypes of RCC (in decreasing frequency): clear cell; papillary; chromophobe; and collecting duct (Eble et al. 2004). The clear cell subtype, also known as conventional RCC, comprises 75–85% of all RCCs and is characterized by its lipid and glycogen-rich cytoplasm. Papillary RCC, also known as the chromophilic subtype, tends to be multifocal and bilateral. It generally has a better prognosis than the clear cell tumors. Chro-

mophobic RCC arises from the cortical collecting duct and is characterized by its large polygonal cells with pale reticular cytoplasm. It also has a better prognosis than clear cell RCC. Finally, the collecting duct subtype arises from the medullary collecting duct, tends to affect younger patients, and often has an aggressive clinical course.

7.2.3 Risk Factors

Renal cell carcinoma typically presents in the sixth and seventh decades of life and is more common in males (two- to threefold increased risk). Risk factors also include cigarette smoking, which doubles risk, obesity, and heavy analgesic use. Diseases associated with RCC are tuberous sclerosis and von Hippel-Lindau disease. Finally, there is increased risk with renal dialysis and with immunosuppression for renal transplants.

7.2.4 Clinical Presentation

Because of its protean and often nonspecific clinical manifestations, RCC is sometimes referred to as the "great imitator" by clinicians. Most common presentations are hematuria (50–60%), pain (40%), and a palpable abdominal or flank mass (30–40%), with the entire triad present in only about 10–20% of patients (Motzer et al. 1996). Patients may also present with a variety of paraneoplastic syndromes, including hypercalcemia, hypertension, erythrocytosis, hyperglycemia, cachexia, anemia, and Stauffer syndrome (nonmetastatic hepatic dysfunction).

7.2.5 Classification

Renal cell carcinoma can be staged with either the Robson or TNM classifications. The Robson classification is the most widely used in imaging literature (Table 7.1; Ergen et al. 2004).

More recently, the American Joint Committee on Cancer (AJCC) and the "Union Internationale Contre le Cancer" (UICC) have devised a TNM-based system for RCC (Guinan et al. 1997). The TNM classification describes the loco-regional extent of disease in greater detail and is more accurate than the Robson classification at predicting survival by stage (Tables 7.2, 7.3).

Table 7.1. Robson renal cell carcinoma classification

Stage I: confined to kidney
Stage II: through renal capsule but confined to Gerota's fascia
Stage IIIA: involvement of renal vein or IVC
Stage IIIB: involvement of local lymph nodes
Stage IIIC: involvement of vessel(s) and nodes
Stage IV: spread to local organs or distant metastases

7.2.6 Therapy

The mainstay of therapy for localized disease is surgery. Radical nephrectomy is the procedure of choice and classically includes resection of the kidney along with all contents within Gerota's fascia including perinephric fat, regional lymph nodes, and the ipsilateral adrenal gland. Nephron-sparing surgery may be an option for patients with small tumors (deKernion 1987). The role of radical nephrectomy in patients with metastatic disease is controversial. Adjuvant radiotherapy does not improve survival, but may be used for palliation in patients who are not surgical candidates.

Despite numerous clinical trials, RCC has proven resistant to all forms of chemotherapy. A review by Yagoda et al. (1995), of over 80 phase-II trials published between 1983 and 1993 testing various cytotoxic agents, showed an overall response rate of only 6%.

Biological agents are another consideration. The observation of occasional spontaneous remissions, the presence of lymphocytes within RCCs, and the results of early clinical trials have prompted the investigation of such agents. Specifically, use of high-dose IL-2 in patients with metastatic RCC showed a 19% response rate (Fisher et al. 2000), though complete and durable response was achieved in only 5% of patients.

7.2.7 New Trends in Detection

"Look and you will find it. What is unsought will go undetected." – Sophocles

Renal cell carcinoma is often identified incidentally. In the past, approximately 10% of RCCs were diagnosed incidentally. Now, with the widespread use of cross-sectional imaging techniques including ultrasound, CT, and MR imaging, this percentage is approximately 36% (Leslie et al. 2003).

Incidental RCCs are typically smaller and of a lower stage and lower grade. These smaller tumors

Table 7.2. The TNM classification

Primary tumor (T)	Regional lymph nodes (N)[a]	Distant metastasis (M)
TX: primary tumor cannot be assessed	NX: regional lymph nodes cannot be assessed	MX: distant metastasis cannot be assessed
T0: no evidence of primary tumor	N0: no regional lymph node metastasis	M0: no distant metastasis
T1: tumor 7 cm or less in greatest dimension limited to the kidney	N1: metastasis in a single regional lymph node	M1: distant metastasis
T2: tumor more than 7 cm in greatest dimension limited to the kidney	N2: metastasis in more than one regional lymph node	
T3: tumor extends into major veins or invades adrenal gland or perinephric tissues but not beyond Gerota's fascia		
T3a: tumor invades adrenal gland or perinephric tissues but not beyond Gerota's fascia		
T3b: tumor grossly extends into the renal vein(s) or vena cava below the diaphragm		
T3c: tumor grossly extends into the renal vein(s) or vena cava above the diaphragm		
T4: tumor invades beyond Gerota's fascia		

[a]Laterality does not affect the N classification

Table 7.3. American Joint Committee on Cancer stage groupings

Stage I	T1, N0, M0
Stage II	T2, N0, M0
Stage III	T1, N1, M0
	T2, N1, M0
	T3a, N0, M0
	T3a, N1, M0
	T3b, N0, M0
	T3b, N1, M0
	T3c, N0, M0
	T3c, N1, M0
Stage IV	T4, N0, M0
	T4, N1, M0
	Any T, N2, M0
	Any T, any N, M1

are usually less biologically aggressive and have a generally slow but variable rate of growth. Bosniak et al. (1995) followed 40 tumors 3.5 cm in diameter or smaller and reported a growth rate of 0.1–1 cm/year (mean 0.36 cm/year).

Not surprisingly, patients with incidentally discovered RCCs have a more favorable prognosis than patients who present with urological symptoms attributable to the tumor. Sweeney et al. (1996) showed a 5-year survival rate of 85% for incidental tumors vs 53% for patients with symptomatic lesions. The overall 5-year survival rate for renal cancer has increased from 45% (1970–1973) to 61% (1989–1996; Landis et al. 1998; Greenlee et al. 2001). This has occurred despite no significant progress in therapy. Lead-time and length biases may play some role in the apparent survival benefits, but the data strongly suggest improved outcomes due to earlier diagnosis; therefore, it appears that progress has been substantial with regard to survival for patients with RCC. Much of this improvement can be attributed to early radiological diagnosis of renal malignancies that in turn has resulted in a higher proportion of tumors that can be cured with surgical resection. For this reason the detection and accurate diagnosis of renal masses are important tasks for radiologists.

7.3 Imaging Modalities

Because of its improved sensitivity and specificity over other imaging modalities, such as intravenous urography and ultrasound (US), contrast-enhanced CT has emerged as the procedure of choice for detecting RCC. Both CT and MR imaging are useful for staging and restaging. In the future, other modalities, such as PET, may also play a significant role.

7.3.1 Plain Radiographs

Occasionally, RCC may be found on an abdominal radiograph, usually appearing as an expansile ball-shaped mass extending from the kidney. Calcifications may also be detected, with approximately 15%

of RCCs containing calcifications that are visible on abdominal radiographs. Gross calcification within any renal mass is worrisome for RCC. Prior to the refinement of cross-sectional imaging, a urology rule-of-thumb was "a calcified renal mass is a surgical renal mass."

Patterns of calcification include thin peripheral rim calcification, irregular central calcification, or a combination of both. Eighty percent of masses on conventional radiography with thin, peripheral rim calcification are benign cysts, and 20% are malignancies, typically cystic RCC. At the opposite end of the spectrum, renal masses that contain central, irregular calcification (Fig. 7.1) are likely to be malignant. Eighty-seven percent of these lesions are RCCs, and the remaining 13% are cysts complicated by previous infection or hemorrhage. Masses that contain both thin, peripheral calcification, and focal, central calcification have a 50% chance of being malignant. Taking all of these variables into account, 60% of renal masses that contain calcium that is visible on an abdominal radiograph, regardless of the calcification pattern, are RCCs (Bracken 1987). Other renal masses that frequently contain calcium are focal xanthogranulomatous pyelonephritis, chronic perirenal hematomas, hemangiomas, aneurysms, and vascular malformations. Cross-sectional imaging allows distinction between benign and malignant calcified renal masses in most patients.

Other plain radiograph findings that may be important are skeletal abnormalities. Renal cell carcinoma often spreads hematogenously to the skeleton, causing lytic skeletal lesions. These lesions sometimes grow slowly and lead to bubbly lesions that focally expand the bone. They can mimic other types of bone lesions, including primary bone neoplasms and myeloma. Finally, patients with tuberous sclerosis, a disease associated with RCC, can have multiple osteomas, which predominate in the skull and spine.

7.3.2 Intravenous Urography

Intravenous urography (IVU) can be performed as follows:

1. Before injection of contrast material, a preliminary radiograph of the abdomen is always obtained.
2. Using bolus technique, 100 ml of 30 mg% contrast material is administered over 30–60 s.
3. One-minute coned radiograph of both kidneys or nephrotomogram.
4. Five-minute coned radiograph of both kidneys. Apply abdominal compression.
5. Ten-minute coned radiograph of both kidneys with abdominal compression, then release compression.
6. Fifteen-minute abdominopelvic plain radiographs, frontal and both obliques.
7. Postvoid abdominopelvic plain radiograph.

It is important to carefully analyze the scout radiograph, particularly for abnormal calcifica-

a

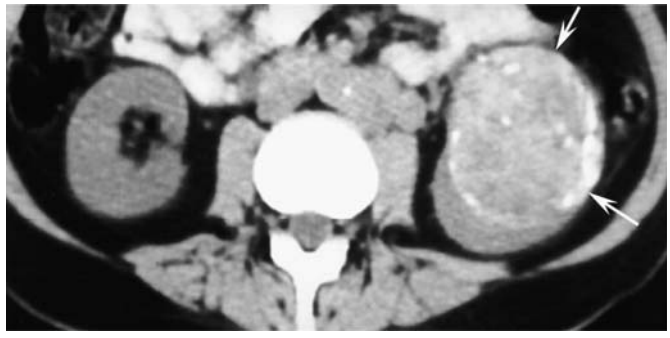

b

Fig. 7.1a,b. Calcifications in RCC in a 56-year-old woman. **a** Anteroposterior cone down radiograph of left upper quadrant demonstrates irregular calcifications (*arrows*) extending from, and projecting over, the lower pole of the left kidney. This pattern is very worrisome for RCC. **b** Axial unenhanced CT scan of same patient demonstrates large, solid RCC (*arrows*) of left kidney. Mass contains numerous calcifications corresponding to those seen on abdominal radiograph.

tions. Renal cell carcinoma is typically expansile and appears as a focal bulge extending from the kidney, displacing normal renal structures (Fig. 7.2). Such contour abnormalities are optimally detected with nephrotomography performed during the nephrogram phase of the IVU. Large masses lead to calyceal splaying, stretching, and draping. Occasionally, an RCC grows predominantly outward and no detectable mass effect is exerted on the calyceal system. Furthermore, RCCs that extend either exclusively anteriorly or posteriorly from the kidney are very difficult to detect with IVU, since the mass contour is obscured by superimposed normal kidney.

Other IVU signs of RCC include notching of the renal pelvis or the ureter, obstruction or invasion of the collecting system, and diminished or absent renal function. Notching results from enlargement of ureteric and renal pelvic vessels, which are recruited to feed or drain an RCC, the majority of which are hypervascular. Focal or diffuse hydronephrosis usually occurs with a large RCC and is due to compression of major calyces, the renal pelvis, or the upper ureter. Less commonly, an RCC grows by infiltration rather than by expansion. In these cases, malignant stricturing of the collecting system may occur secondary to encasement and invasion of the urothelium. Renal cell carcinoma has a predilection for venous extension, which may result in decreased or absent renal function. In fact, the finding of globally decreased function in a kidney with a renal mass is nearly diagnostic of RCC. Less commonly, diminished or absent renal function can result from high-grade ureteral obstruction caused by the RCC compressing the adjacent ureter or from diffuse parenchymal replacement by tumor.

Excretory urography lacks sufficient specificity to accurately characterize renal masses as benign or malignant; therefore, every renal mass detected with or suggested by excretory urography must be imaged with another technique. The most cost-effective approach is to go directly to renal US. With this technique approximately 80% of detected renal masses are characterized as simple cysts, thus ending their diagnostic evaluation (Einstein et al. 1995). The remaining 20% of renal masses require further study with CT or MR imaging.

7.3.3 Ultrasound

The US features of RCC are typical but not diagnostic. Most RCCs appear as expansile, solitary renal masses. They may be hypoechoic, isoechoic, or hyperechoic in comparison with the renal parenchyma, with larger lesions developing heterogeneous echo patterns and internal cystic areas. Most small RCCs are slightly hyperechoic (Fig. 7.3), but approximately one-third are markedly hyperechoic (Fig. 7.4; Forman et al. 1993) and may mimic a benign angiomyolipoma (AML; Fig. 7.5). In distinguishing the two, the ultrasound findings of an anechoic perimeter or internal cystic areas strongly favor RCC, though CT or MR imaging is required for

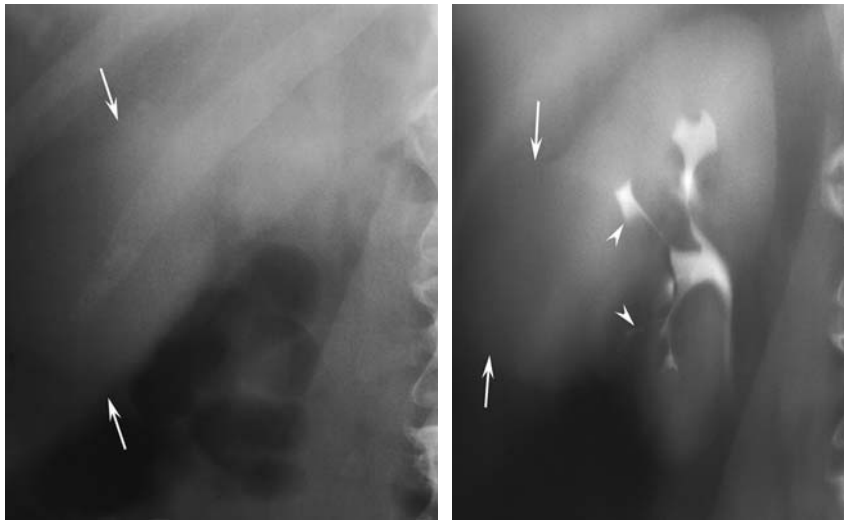

a **b**

Fig. 7.2a,b. Renal mass in a 49-year-old woman. **a** Anteroposterior scout abdominal radiograph shows contour abnormality (*arrows*) along lateral aspect of right kidney. **b** Anteroposterior nephrotomogram shows mass (*arrows*) with splaying of collecting system (*arrowheads*).

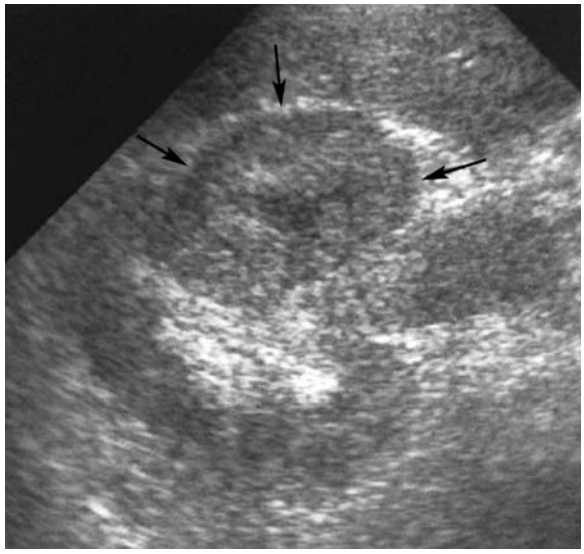

Fig. 7.3. Renal cell carcinoma in a 55-year-old man. Axial US image demonstrates expansile right renal mass (*arrows*). This mass is slightly hyperechoic and heterogeneous compared with normal renal parenchyma. These features are typical of most RCC.

further characterization (Yamashita et al. 1993). Both CT and MR imaging are exquisitely sensitive for the detection of intratumoral fat, the presence of which is highly suggestive of AML (Fig. 7.5; Takahashi et al. 1993) and excludes an RCC except in the rare case that the tumor has grown to engulf normal renal sinus or perirenal fat.

Another interesting US feature is the capacity to demonstrate the internal architecture of renal tumors better than other imaging techniques. Some renal masses appear cystic or homogeneous with CT and MR imaging. Ultrasound examination of these lesions may demonstrate complex internal components with septations, fronds of solid tissue lining the periphery of the mass, or other evidence of malignancy; therefore, US may be used as an adjunctive test when CT findings are equivocal. In particular, US may be useful when CT findings suggest a cystic lesion not clearly a simple cyst but not obviously malignant (Fig. 7.6).

An infiltrating RCC may cause only subtle US abnormalities or none at all, but may lead to second-

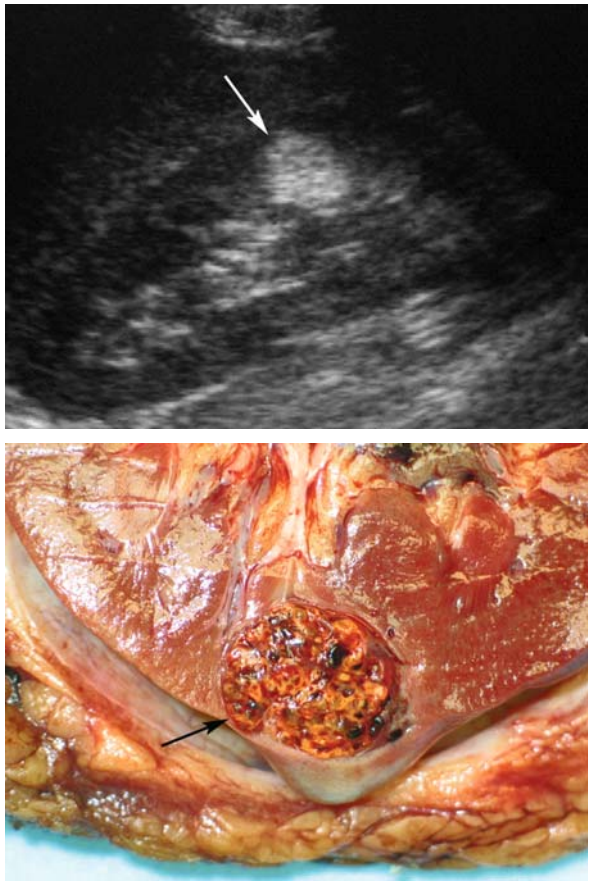

a

c

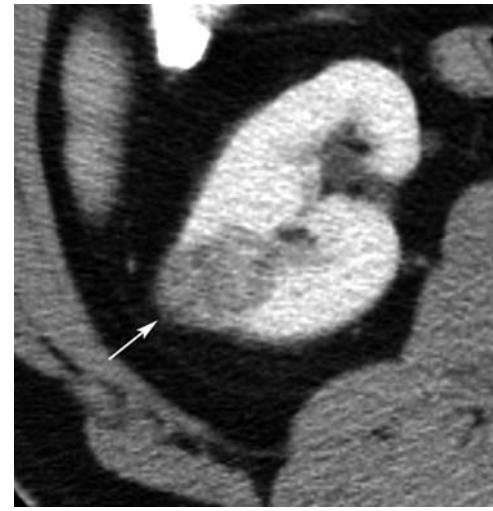

b

Fig. 7.4a-c. Renal cell carcinoma in a 66-year-old woman. **a** Longitudinal US image reveals markedly hyperechoic renal cell carcinoma (*arrow*) indistinguishable from angiomyolipoma. **b** Axial contrast-enhanced CT scan reveals solid enhancing lesion (*arrow*) with no detectable fat. **c** Pathology specimen shows yellow-orange mass (*arrow*) with spongy consistency and areas of hemorrhage. Final diagnosis was conventional RCC.

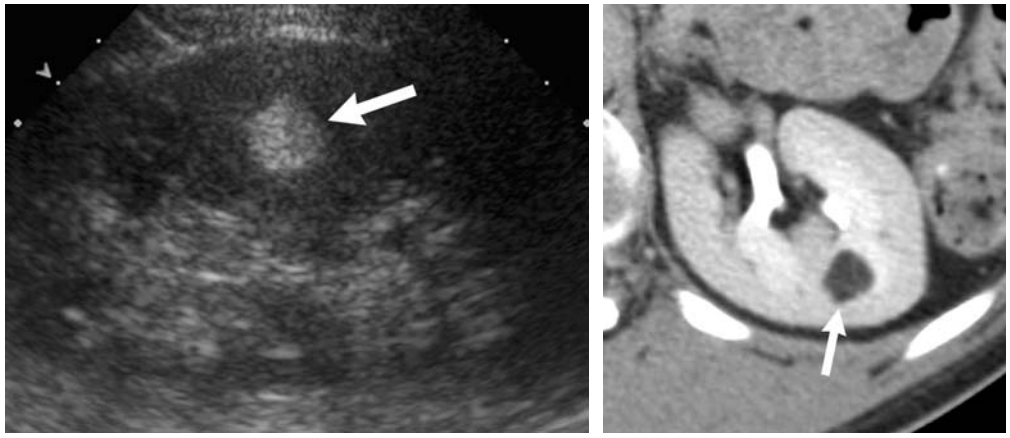

Fig. 7.5a,b. Angiomyolipoma in a 41-year-old woman. **a** Longitudinal ultrasound image shows small hyperechoic lesion (*arrow*) within renal parenchyma typical of angiomyolipoma. **b** Axial contrast-enhanced CT scan reveals fat density within lesion, confirming diagnosis (*arrow*).

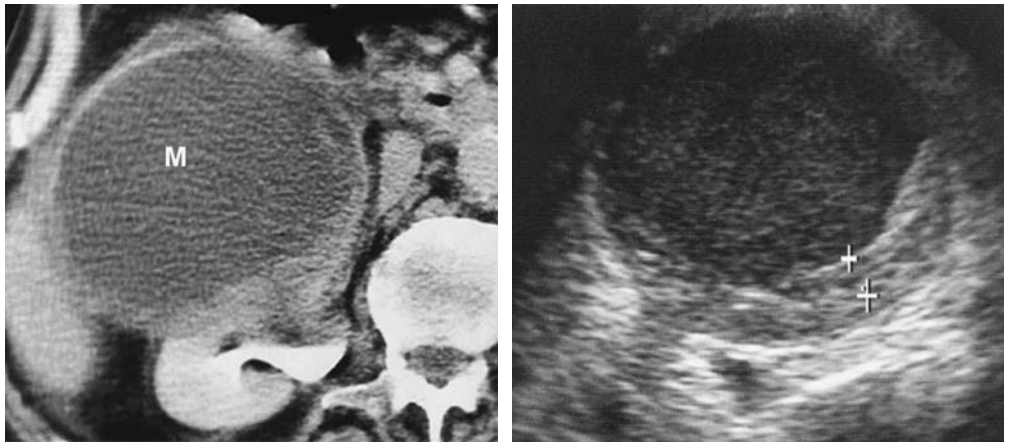

Fig. 7.6a,b. Papillary RCC in a 44-year-old man. **a** Axial contrast-enhanced CT scan demonstrates renal mass (*M*). Most of mass appears cystic. **b** Axial US image through right kidney in this patient better demonstrates thick rind of solid tissue. The cystic component contains many low-level echoes and this component of mass is not simply cystic.

ary abnormalities, including hydronephrosis and vascular encasement with diminished Doppler flow to the area of involvement. Alteration of the normal central sinus echo complex may also be seen.

Ultrasound is less accurate than either CT or MR imaging for staging RCC. Ultrasound should not be used as the sole modality for staging RCC, but it may be a helpful adjunct to other imaging techniques. The major limitations of US in staging RCC are the inability to image the renal vein and the subhepatic inferior vena cava reliably, and limited detection of abdominal lymphadenopathy. For staging, it is used mainly as an adjunct examination when tumor extension into the inferior vena cava is detected with CT but the exact superior extent of the tumor thrombus cannot be determined with CT. In these cases, US is highly accurate (95%) in determining whether tumor thrombus extends into the intrahepatic inferior vena cava (Fig. 7.7; Gupta et al. 2004). This portion of the inferior vena cava can be visualized with US in 100% of cases, and tumor thrombus in this region is identifiable whenever present. Although this area can also be evaluated with either MR imaging or venography, US is the most cost-effective technique to resolve this isolated staging problem.

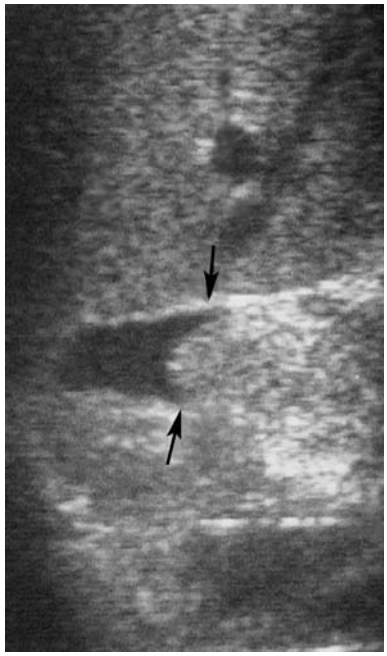

Fig. 7.7. Tumor extension into the inferior vena cava in a 66-year-old man. Longitudinal transabdominal US image demonstrates upper extent of a RCC (*arrows*) within intrahepatic inferior vena cava.

7.3.4 Angiography

Renal angiography, once a basic element in the diagnosis of renal masses (Watson et al. 1968), is now of little value. Angiography has traditionally been reserved for mapping vascular supply to the kidney harboring a renal mass when a partial nephrectomy is contemplated. Since noninvasive techniques, such as CT or MR angiography, can be used to derive similar information, these techniques have largely replaced catheter angiography for this indication at most centers.

Renal arteriography in concert with embolization may be useful in the treatment of some RCCs. Tumor embolization can reduce intraoperative blood loss, or can diminish symptoms in patients considered inoperable. In rare cases, angiography may be useful to distinguish among various renal masses. In particular, angiography may be an alternative to open biopsy in the evaluation of infiltrating renal neoplasms, the differential diagnosis for which includes urothelial neoplasm, inflammatory lesion, infarct, or infiltrating RCC. Each of these entities, except RCC, is nearly always hypovascular or avascular; therefore, an infiltrating renal mass that is hypervascular strongly suggests an infiltrating RCC. This finding is important as RCC is traditionally treated with nephrectomy, whereas transitional cell carcinoma is treated with nephroureterectomy, and many other infiltrating lesions are treated medically.

7.3.5 Cross-Sectional Imaging

7.3.5.1 Protocols

Conventional renal CT can be performed as follows:

1. Oral contrast (dilute Gastrografin or barium) is utilized.
2. Intravenous contrast is utilized with injection of 125 ml of 30 mg% contrast medium at a rate of 2–4 ml/s.
3. Evaluation should include contiguous 2.5-mm sections through the kidneys with unenhanced and contrast-enhanced sequences. Five-millimeter sections can be used elsewhere in the abdomen/pelvis.
4. The kidneys should be scanned during the corticomedullary phase (70 s) and the tubular/nephrographic phase (120 s).
5. A CT angiogram can also be obtained obviating the need for later catheter angiography for surgical planning. This requires initial scanning during the arterial phase (25 s).

Magnetic resonance imaging of the kidney can be performed as follows:

1. Unenhanced and contrast-enhanced T1-weighted spin-echo or gradient-echo images in the axial and coronal planes are recommended. An image section thickness of 5–7 mm is recommended. Prior to contrast administration and immediately afterward, breath-hold 3D fast spoiled gradient-echo images, with 4 mm or less section thickness, should be obtained. The torso phased-array coil is used routinely to image the kidneys.
2. Fast spin-echo T2-weighted images of the kidneys in the axial or coronal plane are obtained. These images are usually supplemented with a heavy T2-weighted sequence such as single-shot fast spin-echo (SSFSE, General Electric) or half-Fourier acquisition single-shot turbo spin echo (HASTE, Siemens).
3. The liver, adrenal glands, and upper retroperitoneum should also be evaluated routinely.

4. Flow-compensated T1-weighted spoiled gradient-echo images are used to evaluate patency of the renal veins and inferior vena cava. This pulse sequence can be implemented alone or as a component of MR venography.

7.3.5.2 Diagnosis

With CT or MR imaging alone, RCC can be diagnosed with better than 95% accuracy (Bechtold and Zagoria 1997). In our own experience with CT, 94% of RCCs are detected as expansile masses, whereas the remaining 6% grow by infiltration without significant disruption of the reniform shape of the involved kidney (Gash et al. 1992). The precontrast density of RCC compared with the background renal parenchyma can be hypodense, isodense, or hyperdense. Hyperdensity presumably results from acute hemorrhage, calcium, or proteinaceous debris within the tumor. Almost half of RCCs display a transient hyperdense blush during bolus contrast material injection (Fig. 7.8).

Note that the above CT protocol calls for imaging both during the corticomedullary phase (which also corresponds to the portal venous phase of liver enhancement) and the tubular phase of renal enhancement. Dual-phase imaging is important because during the corticomedullary phase, where renal parenchymal enhancement predominates in the cortex, there is decreased conspicuity of hypervascular cortical tumors and similar decreased conspicuity of hypovascular medullary tumors. The optimal phase for renal mass detection with helical CT is during the tubular phase (Zagoria et al. 1990). Again, this typically occurs about 120 s after the initiation of intravenous contrast material injection. Virtually all renal tumors appear less dense than enhanced renal parenchyma during this phase of enhancement.

Tumor homogeneity, distinctness of the RCC–kidney interface, and the shape and sharpness of the tumor margins are largely dependent on tumor size. The RCCs less than 5 cm in diameter are usually homogeneous masses with a distinct mass–kidney interface and smooth, sharp margins (Fig. 7.9). These features are rare in large RCCs, which usually display malignant findings, including central necrosis as a result of inadequate vascular supply, marginal lobulation reflecting differential growth rates within the tumor, infiltration of surrounding tissues including the renal collecting system (Fig. 7.10), and

Fig. 7.8. Transient hyperdense blush in a 68-year-old man with RCC. Axial CT scan taken during a bolus injection of intravenous contrast material demonstrates expansile right renal mass (*arrows*). This mass enhances slightly greater than does normal renal parenchyma. This feature is commonly seen with hypervascular RRC.

Fig. 7.9. Small RCC in a 58-year-old man. Axial contrast-enhanced CT scan demonstrates homogenous renal mass *(M)* which has a distinct interface with normal enhancing renal parenchyma. This feature is typically seen with small RCC. The 4-cm mass was proven to be RCC.

production of an indistinct mass–kidney interface (Fig. 7.11). Calcifications are visible by CT in 31% of RCCs (Zagoria et al. 1990) and are more common in papillary (32%) and chromophobe (38%) RCCs than in conventional RCC (11%; Kim et al. 2002).

Thus far, the major role of MR imaging in RCC evaluation lies in staging of cases deemed indeterminate after CT evaluation or in imaging patients in whom obtaining optimal CT scans is impossible. The MR imaging characteristics of RCC are similar to those described for CT. With gadolinium injection, as with iodinated contrast material injection for CT, RCCs enhance and become conspicuous within the renal parenchyma. A recent study showed that

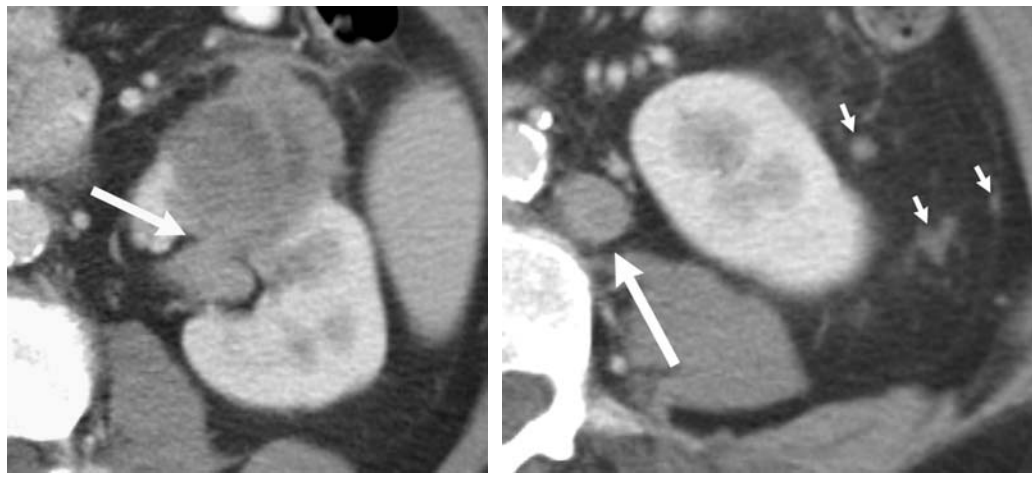

Fig. 7.10a,b. Renal cell carcinoma in a 57-year-old man. **a** Axial contrast-enhanced CT image shows large exophytic solid mass with invasion into renal collecting system (*arrow*). **b** Axial CT scan at different level shows enlarged para-aortic lymph node (*large arrow*) and small perinephric nodules (*small arrows*), both suspicious for malignant involvement.

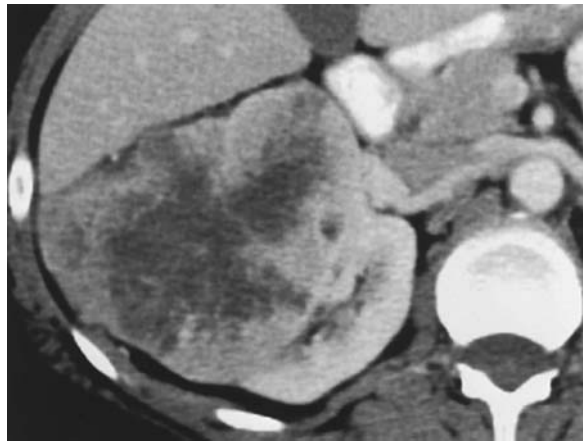

Fig. 7.11. Large RCC in a 61-year-old woman. Axial contrast-enhanced CT scan shows a large right RCC demonstrating features typical of larger RCC. Heterogeneity with central necrosis, irregular margins, and indistinct interface with normal kidney are all demonstrated in this renal mass.

enhancement of a renal mass of greater than 15% on scans made 3–5 min after gadolinium injection is strongly suggestive of a malignancy (Ho et al. 2002). This measurement of enhancement is predicated on the fact that all imaging parameters are set exactly the same before and after gadolinium injection. Gadolinium injection also improves the imaging quality of MR renal angiograms, if they are obtained early after bolus injection. Magnetic resonance imaging is particularly useful for the diagnosis of RCC in patients for whom iodinated intravascular contrast media present a significant health risk, such as patients with a history of a major adverse reaction or those with renal insufficiency. Although gadolinium is more nephrotoxic than iodinated contrast materials on a milliliter-to-milliliter basis, at the smaller doses required for MR imaging it is safe in patients with renal insufficiency.

Infiltrating RCCs, an uncommon subtype, do not substantially alter the reniform shape of the kidney, and these lesions often have homogeneous internal architecture (Fig. 7.12). They are detectable mainly because of their hypodensity compared with surrounding parenchyma on contrast-enhanced CT or MR imaging. Without the use of other diagnostic modalities, such as angiography or biopsy, these tumors may be indistinguishable from invasive urothelial malignancies.

Renal cell carcinomas sometimes appear cystic, and about 22% of proven RCCs are predominantly cystic (Zagoria et al. 1990); these are discussed in section 7.4.1.

7.3.5.3 Staging

Once RCC is suspected, staging is critical for appropriate treatment planning. It is often impossible to differentiate between stage I and stage II RCC with CT and MR imaging. Although this distinction does affect prognosis, it traditionally does not affect management, since radical nephrectomy is the treatment of choice in either case. More recently, a growing number of surgeons are treating early-stage

Fig. 7.12a,b. Typical CT appearance of infiltrating renal mass in a 69-year-old man. **a** Axial unenhanced CT scan shows infiltrating mass in the right kidney (*arrow*) which is barely discernable as a subtle hypodense area. **b** Axial contrast-enhanced CT scan shows a readily identifiable geographic area of decreased enhancement (*arrow*). Typical of infiltrating lesions, this RCC does not grossly affect bean shape of kidney.

RCC with partial nephrectomy or tumorectomy (Ljungberg 2004). Results indicate that partial nephrectomy is as effective a treatment for both stage I and stage II RCC as radical nephrectomy. When partial nephrectomy is being considered, it is important to scrutinize the ipsilateral adrenal gland for evidence of tumor involvement. When present, this form of stage II RCC will necessitate adrenalectomy in conjunction with tumor removal; otherwise, the adrenal gland is spared.

Some signs have been considered suggestive of extracapsular (stage II) tumor spread. These signs include visualization of the following features in the perinephric space: fat obliteration; collateral vessels; stranding or cobwebbing; fascial thickening; and discrete soft tissue masses. Obliteration of perinephric fat and visualization of perinephric collateral vessels are not reliable signs of stage II disease, and their significance for staging is minimal. Fat obliteration indicates only mass effect, not invasion, in the perinephric space, and collateral vessels form in response to tumor angiogenesis factor, but do not indicate extension of tumor. Likewise, perinephric stranding should not be considered a sign of extracapsular tumor spread. Perinephric stranding results from thickening of perinephric septa by edema, inflammation, or vascular congestion. Although fascial thickening is in fact often due to direct tumor spread, it may also occur as a result of reactive edema or hyperemia. The most reliable imaging sign of RCC spread to the perinephric space is the presence of a discrete perinephric soft tissue mass. The presence of a focal perinephric mass larger than 1 cm in diameter is strongly indicative of stage II RCC; however, this finding is seen in less than half of patients with stage II disease. To date, reliable differentiation between stage I and stage II disease remains in the domain of the pathologist.

With MR imaging, as with CT, no reliable criteria have been established for differentiating between stage I and stage II RCC. Because they are multiplanar, MR images can be helpful in determining the presence of adjacent organ invasion when this remains unclear after CT and US. Sagittal and coronal images are usually definitive in excluding the presence of direct adjacent organ invasion when a fat plane exists between the RCC and that organ. Altered signal characteristics within adjacent organs must be interpreted with care when they are the sole abnormality, as signal changes in compressed segments of liver, for example resulting from congestion and edema, may mimic changes of direct invasion.

Often the most difficult imaging task with CT is accurate evaluation of tumor extension into the renal vein. After power-injected contrast material administration, thin (5 mm or less) CT slices made through the level of the renal vein will yield 95% accuracy in detecting renal vein thrombus complicating RCC (Welch and LeRoy 1997). Secondary signs of renal vein involvement are unreliable. Renal vein enlargement and displacement are not accurate indicators of venous invasion, as the renal vein is often enlarged simply due to the high flow of blood from a hypervascular RCC. Venous displacement may reflect distortion of its normal course from a bulky renal tumor or displacement from extrinsic nodal disease. The normal left renal vein may have an abrupt caliber change as it crosses between the

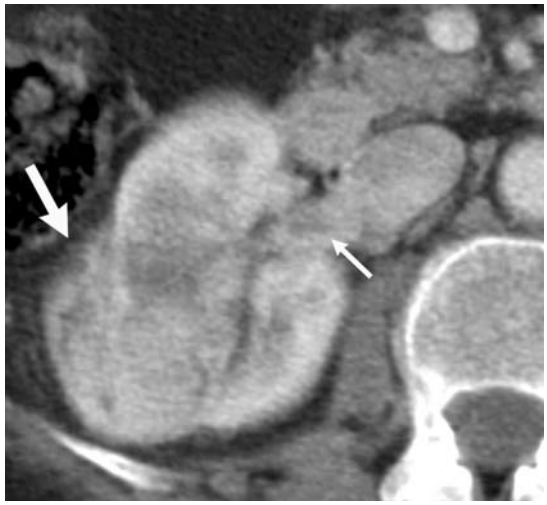

Fig. 7.13. Tumor extension into renal vein in a 54-year-old woman with RCC. Axial contrast-enhanced CT scan shows solid mass (*large arrow*) and filling defect (*small arrow*) in the renal vein compatible with tumor extension.

superior mesenteric artery and aorta; elsewhere such changes usually indicate the presence of tumor thrombus. The most reliable sign of tumor invasion is direct visualization of the hypodense thrombus in an otherwise opacified vein (Fig. 7.13). These criteria also apply to the diagnosis of tumor thrombus in the inferior vena cava.

The degree of venous tumor extension is also accurately depicted with multiplanar MR imaging (Fig. 7.14). Venous extension of tumor thrombus is well demonstrated with standard spin-echo T1-weighted images, on which flowing blood appears black because of signal void, with relative increased signal of the tumor thrombus. Alternatively, low-flip-angle gradient-echo scans enhance the signal of flowing blood. The resulting "bright-blood" images are similar in appearance to inferior vena cavograms and renal vein phlebography; thrombus appears as a hypointense filling defect surrounded by the hyperintensity of flowing blood. Tumor extension at or

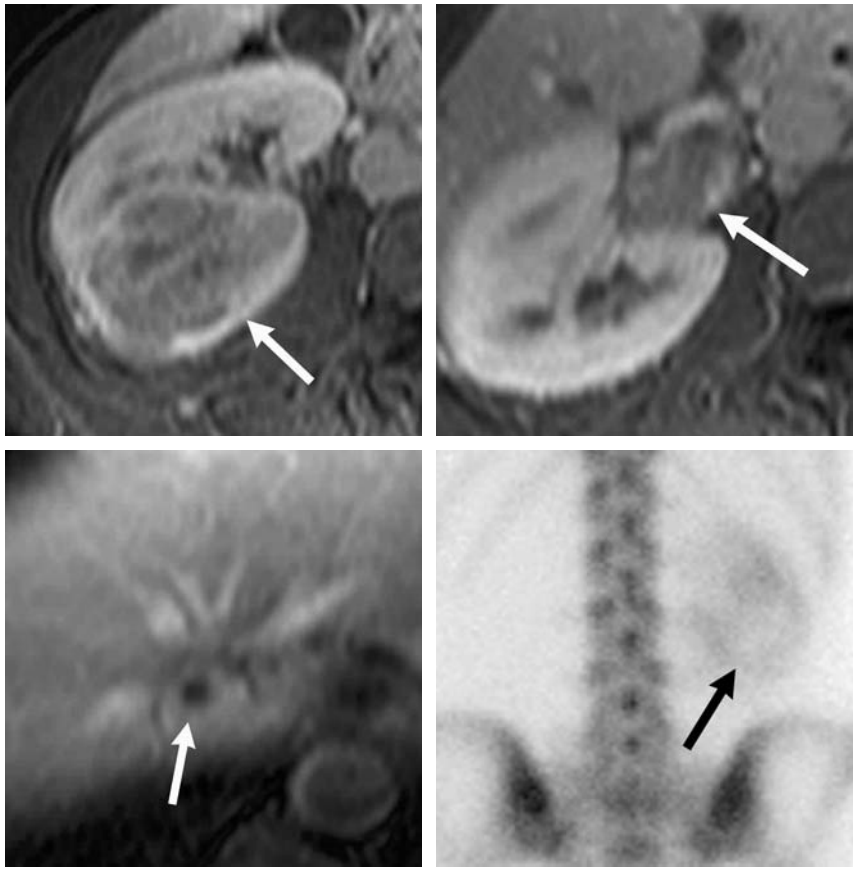

Fig. 7.14a-d. Venous involvement in a 72-year-old man with RCC. Axial contrast-enhanced fat-suppressed T1-weighted MR images show **a** RCC (*arrow*), **b** extension of tumor into renal vein (*arrow*), and **c** extension within inferior vena cava to level of hepatic veins (*arrow*). **d** Staging bone scan (posterior view) incidentally shows the right renal mass as an area of photopenia (*arrow*). The left kidney was surgically absent.

above the level of the hepatic veins dictates the surgical approach. If the tumor does not extend beyond hepatic inflow, an abdominal approach may be used for tumor excision and thrombectomy. Extension above this level necessitates an intrathoracic approach, and requires intraoperative cardiopulmonary bypass.

Clotted blood, also known as bland thrombus, may develop in veins adjacent to tumor thrombus, and the appearance may suggest more extensive tumor thrombus than is actually present. Both CT and MR imaging can be used to differentiate bland thrombus from tumor thrombus only when neovascularity (Fig. 7.15) or substantial contrast enhancement is detectable within the tumor thrombus (Fig. 7.16).

Both CT and MR imaging are very effective in detecting retroperitoneal lymphadenopathy. Nodes 1.5 cm or larger in short axis are pathologically enlarged and therefore suggestive of lymphatic metastases. This criterion assures accurate detection of most nodal metastases. Unfortunately, malignant lymphadenopathy cannot be differentiated from lymph node enlargement due to reactive

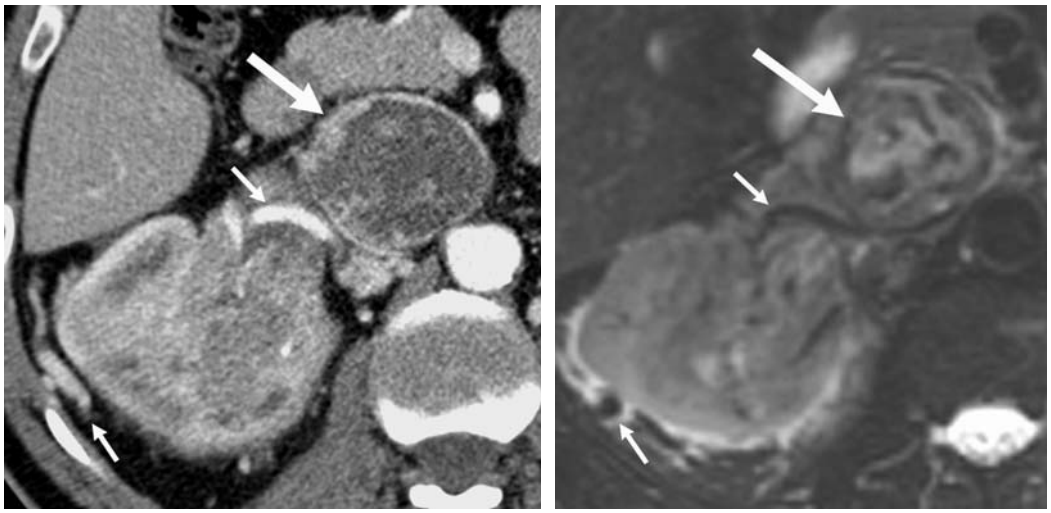

Fig. 7.15a,b. Neovascularity within tumor thrombus in a 54-year-old man with RCC. **a** Axial contrast-enhanced CT scan shows tumor thrombus extending into renal vein and distended inferior vena cava (*large arrow*). Tumor neovascularity in tumor thrombus and perinephric vessel enlargement are also noted (*small arrows*). **b** Axial T2-weighted MR image again shows the inferior vena cava thrombus (*large arrow*). Thrombus neovascularity and perinephric vessel enlargement are identified as flow voids (*small arrows*).

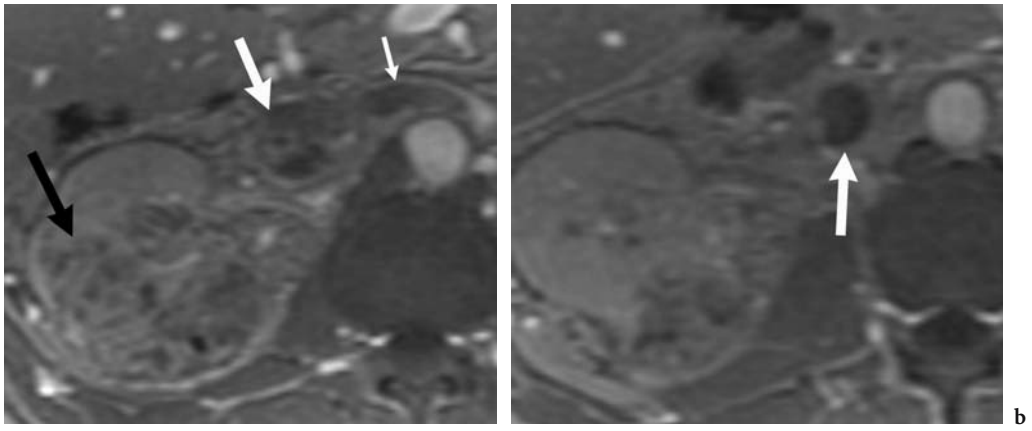

Fig. 7.16a,b. Bland thrombus and tumor thrombus in a 39-year-old man with RCC. Axial delayed contrast-enhanced fat-suppressed T1-weighted MR images show **a** renal mass (*black arrow*), enhancing tumor thrombus within inferior vena cava (*large white arrow*), and non-enhancing filling defect within left renal vein (*small white arrow*) compatible with bland thrombus. **b** Similar bland thrombus is identified in more inferior aspect of the inferior vena cava (*arrow*).

hyperplasia. Reactive hyperplasia in regional nodes is more commonly seen with RCCs complicated by tumor necrosis and venous extension. Also, nodes in the 1- to 1.5-cm range, particularly if they are more numerous than expected, are considered indeterminate but suspicious for spread of malignant disease. Occasionally, normal-sized nodes (<1 cm) harbor microscopic tumor foci.

Distant metastases to liver and bone are generally easy to identify with CT or MR imaging. Organ-appropriate window settings of scans should be done in all cases to maximize the CT visualization of metastatic deposits. Since RCC metastases are often hypervascular, making them difficult to detect in the enhanced liver, CT images of the liver during the hepatic arterial phase of liver enhancement are helpful in identifying many of these lesions. With MR imaging, metastatic deposits in the liver can be readily detected and distinguished from benign hemangiomas and cysts. Metastases to the spleen can be very difficult to identify because of the MR imaging characteristics of the spleen, which can mask focal tumors. Finally, MR imaging may be more sensitive than CT in the detection of unsuspected bony metastases because of its exquisite bone marrow imaging capability.

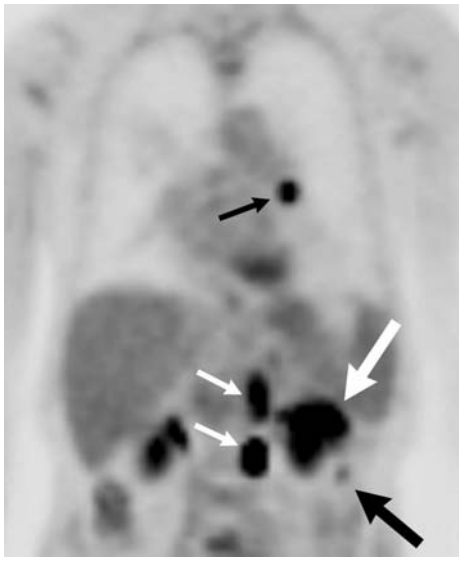

Fig. 7.17. Metastatic survey in a 61-year-old man with RCC. Coronal FDG-PET image shows increased radiotracer uptake in large left renal mass (*large white arrow*), perinephric focus (*large black arrow*), para-aortic lymph nodes (*small white arrows*), and left hilar lymph node (*small black arrow*). all compatible with metastatic disease.

7.3.6 PET Imaging

Oncological PET imaging with F-18 deoxyglucose (FDG) is predicated on the increased glucose utilization exhibited by tumor cells. Regarding the diagnosis of primary lesions, FDG-PET is limited by physiological radiotracer uptake in the kidney as well as by overall modest uptake within the tumor itself. Regarding staging and restaging, the overall sensitivity of FDG-PET (64–71%) in the detection of metastatic foci is limited (Majhail et al. 2003; Jadvar et al. 2003). FDG-PET may play a complementary role in the restaging of RCC patients related to superior specificity and positive predictive value compared with conventional imaging (Fig. 7.17; Kang et al. 2004).

7.4 Additional Considerations

7.4.1 Cystic Renal Cell Carcinoma

Cystic renal masses have been studied extensively with CT and US. The Bosniak classification system is useful for categorizing these lesions as to their etiology and serving as a guide for treatment (Bosniak 1997). It is summarized as follows:

1. Class I lesions are simple cysts. Findings that are diagnostic of a simple renal cyst include a water-density mass that does not enhance and has an imperceptible or barely perceptible peripheral margin. Ultrasound findings include an anechoic lesion with thin walls and increased through-sound transmission (Fig. 7.18).
2. Class II lesions have thin septation(s) (Fig. 7.19), thin peripheral calcifications, are non-enhancing hyperdense cysts, or have features typical of infected cysts. With CT, one can be reasonably confident that these class II lesions are benign; however, they do merit follow-up CT scanning in 6–12 months to exclude progression. Septations and hyperdense internal material are thought to develop after cyst infection or hemorrhage, which leads to the development of fibrinous internal septa, dystrophic calcifications in the wall of the cyst, or internal proteinaceous material reflected by hyperdensity on unenhanced CT scans. The hyperdense cysts are the most problematic for radiologists. These lesions appear to be of higher

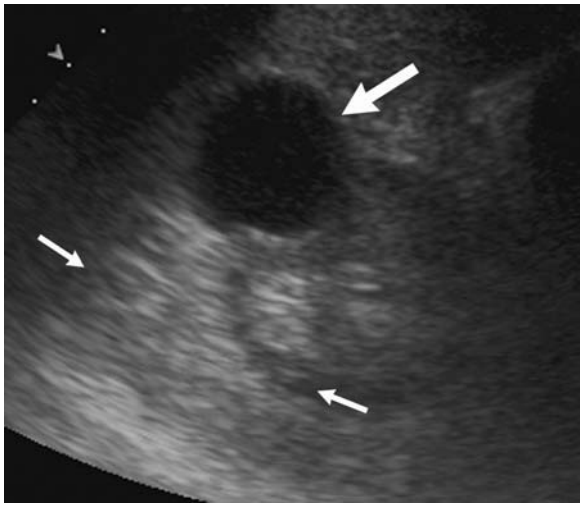

Fig. 7.18. Bosniak I lesion in a 37-year-old woman. Axial US image shows anechoic lesion (*large arrow*) with thin walls and evidence of increased through-sound transmission (*small arrows*) confirming simple cyst.

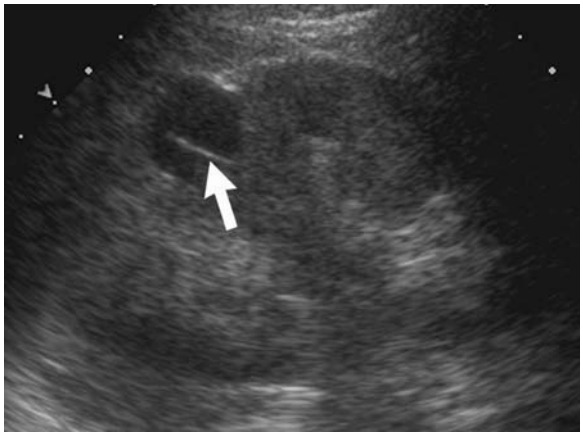

Fig. 7.19. Bosniak II lesion in a 40-year-old woman. Longitudinal US image shows cyst with single thin septation (*arrow*).

density than the kidney on unenhanced CT. With contrast infusion, they appear hypodense to the enhanced renal parenchyma, and there is no interval enhancement of these lesions with contrast material injection. Management of these lesions is somewhat controversial. Although the lack of enhancement seems to indicate that these are benign lesions, some researchers believe that US of these lesions is helpful in confirming that they are benign, albeit complicated, cysts. Unfortunately, these lesions often contain internal echoes when imaged with US. In such cases, follow-up imaging or even surgical extirpation may be necessary. Since the overwhelming majority of these lesions are benign, follow-up CT seems to be the more prudent approach. If these lesions contain enhancing components, they are not class II lesions, but rather class IV lesions, and surgical removal is indicated.

3. Class III lesions have more complex imaging characteristics, including dense, thick calcifications, numerous septa or multiple locules, septal nodularity, or solid components that do not enhance. Approximately one-half of these lesions are cystic RCCs; the remainder are benign lesions such as cysts complicated by infection or hemorrhage, or the benign tumor known as multilocular cystic nephroma. There is no reliable way to distinguish among these lesions without surgery. Since many of them are benign, renal-sparing surgery can be considered for these patients, but surgical excision is generally recommended for complex cystic masses. Magnetic resonance imaging may be helpful in evaluating cystic lesions that are equivocal by US and CT (Fig. 7.20).
4. Class IV lesions are always considered malignant. The major criterion of a class IV lesion is an area of enhancing solid tissue. With cystic neoplasms, this tissue often is at the periphery, and enhancement may be subtle (Fig. 7.21). Careful comparison of the margins of the cystic mass between the unenhanced and the contrast-enhanced CT scan may reveal an area of enhancement. If so, the lesion should be presumed to be RCC and surgery is indicated.

As stated previously, approximately 20% of RCCs are predominantly cystic on CT or MR imaging. Three-quarters of these are solid RCCs that have undergone central liquefaction necrosis. With growth, these lesions tend to outstrip their blood supply, and central areas become ischemic and necrotic. The remaining lesions are truly cystic RCCs. This subgroup usually has a papillary cellular growth pattern, which has been associated with a decreased rate of metastases and better prognosis than other forms of RCC. Papillary RCCs are also often multifocal and may be familial. These tumors tend to be slow-growing masses with fronds of tissue protruding centrally from the margins. Fluid may be a large component of these masses. They are usually hypovascular, even after attaining a large size. Although these lesions may have subtle features indicating their true nature on CT, US often better demonstrates the complex internal architecture (Fig. 7.6) typical of a papillary RCC.

Cysts may be associated with renal malignancies in other ways. Since renal cysts are quite common,

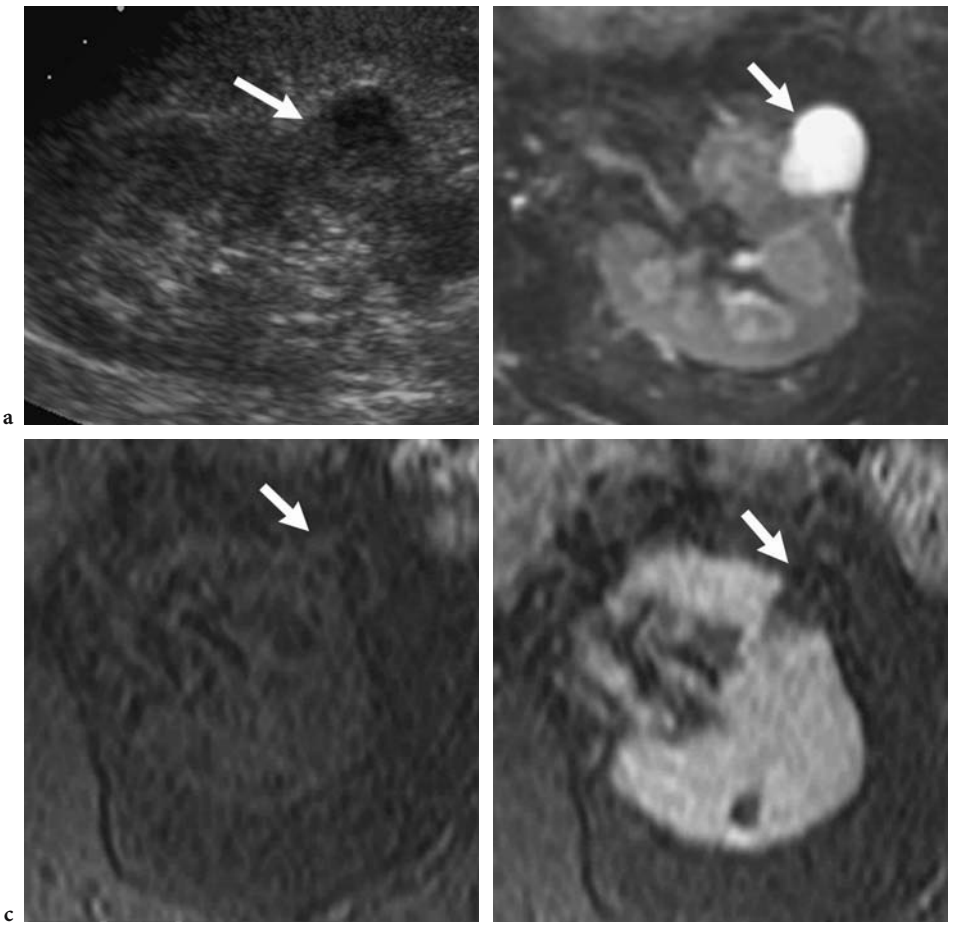

Fig. 7.20a-d. Cystic lesion in a 44-year-old man. **a** Longitudinal US image shows exophytic cystic lesion with ill-defined margins and questionable solid component (*arrow*). **b–d** Axial MR images show the lesion (*arrow*) to be homogeneous and hyperintense on T2-weighted image (**b**) and hypointense on unenhanced fat-suppressed T1-weighted image (**c**). There is no evidence of enhancement on contrast-enhanced fat-suppressed T1-weighted image (**d**). These findings are compatible with benign lesion.

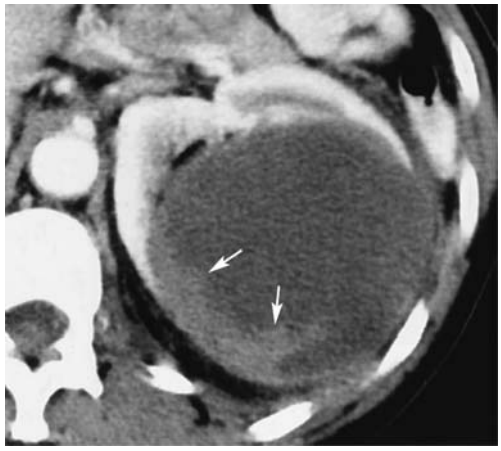

Fig. 7.21. Suspicious cystic renal mass in a 58-year-old man. Axial CT scan of this papillary RCC demonstrates solid tissue with subtle peripheral enhancement (*arrows*). Enhancing tissue in a cystic renal mass strongly suggests a malignant tumor.

cysts and tumors may occur in the same kidney and yet be causally unrelated. A renal tumor may occur adjacent to a solitary or dominant cyst. This pattern of abnormalities is likely related and occurs because the neoplasm obstructs renal tubules and causes dilatation and cyst formation. Since recognition of these cysts may lead to detection of the nearby renal tumor, these focal, solitary cysts are sometimes referred to as "sentinel" cysts. Some conditions cause formation of both renal cysts and renal neoplasms. This category includes von Hippel-Lindau disease (Choyke et al. 1990; Jennings and Gaines 1988), tuberous sclerosis (Seidenwurm and Barkovich 1992), and long-term dialysis (Siegel et al. 1988). Finally, the rarest cyst–renal neoplasm association is the formation of an RCC in the wall of a preexisting simple renal cyst. Once sizable, these neoplasms can be detected with US, CT, or MR imaging as a

solid nodule originating in the wall of cyst. The solid component of such a mass usually enhances with contrast material injection, and these tumors are managed identically to other RCCs.

7.4.2 Differential Diagnosis of Renal Masses

Several entities may mimic RCC; these include complex cysts, AML, abscess, metastases, oncocytoma, multilocular cystic nephroma (MLCN), and focal xanthogranulomatous pyelonephritis (XGP). Complex cysts and AML are discussed in section 7.4.1 and section 7.3.3, respectively.

Fig. 7.22. Renal abscess in a 59-year-old woman. Axial contrast-enhanced CT scan shows hypodense lesion (*arrow*) with ill-defined margins in the right kidney. Distinction from RCC was made based on clinical presentation and follow-up.

Renal abscesses usually result from inadequate treatment of pyelonephritis, which leads to central liquefaction and formation of a discrete intrarenal lesion. Abscesses, when visible, appear as thick-walled cystic masses on IVU or US. With CT, abscesses appear as rounded, well-defined, low-density masses with central liquefaction (Fig. 7.22). Distinction from RCC is based on clinical presentation. Rarely, patients present with a true renal abscess but have an underlying RCC. In these cases, the necrotic tumor center becomes secondarily infected. Follow-up renal imaging studies of patients with renal abscess, after resolution of their symptoms, are necessary to exclude an occult RCC.

Occasionally, a solitary renal metastasis or solitary focus of renal lymphoma may occur. In a patient with known extrarenal malignancy, percutaneous biopsy or surgical biopsy is usually necessary to distinguish RCC from a solitary metastasis. Primary sources that account for most renal metastases include carcinoma of the breast, lung, gastrointestinal tract, or malignant melanoma. Also, lymphoma commonly spreads to the kidneys, but true primary renal lymphoma is extremely rare.

Oncocytomas are benign renal tumors, comprising 5% of resected renal masses (Schatz and Lieber 2003), and having no metastatic potential. Unfortunately, preoperative diagnosis is often impossible since imaging characteristics of these lesions substantially overlap with those of RCC (Fig. 7.23). In addition, biopsy is of little value, since

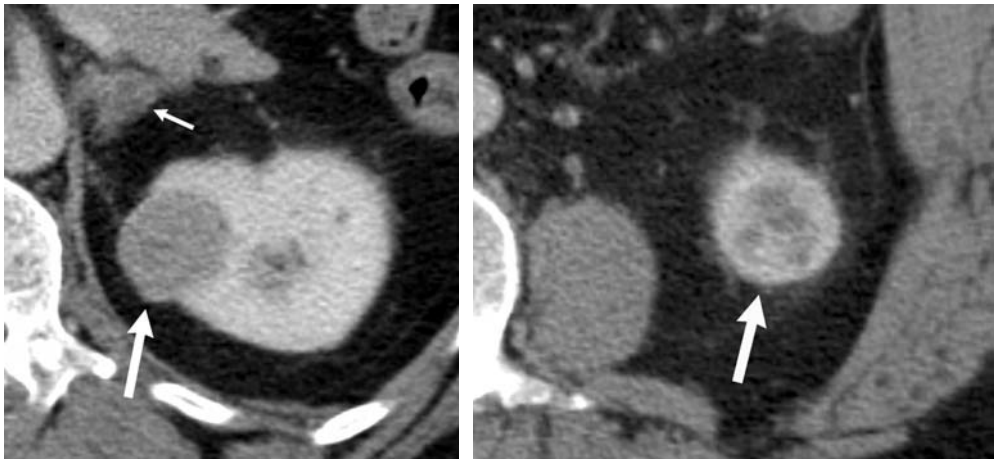

a **b**

Fig. 7.23a,b. Oncocytoma and RCC in a 44-year-old man. **a** Axial contrast-enhanced CT scan shows solid enhancing mass (*large arrow*) in the left mid-kidney and suspicious para-aortic lymph node (*small arrow*). This mass was proved to be RCC. **b** Axial contrast-enhanced CT scan caudad to **a** shows a second solid enhancing left kidney lesion (*arrow*) which proved to be oncocytoma.

some RCCs contain benign-appearing oncocytic elements that are indistinguishable from an oncocytoma. On IVU, oncocytomas are often large at initial detection and have very smooth margins. The US findings are nonspecific. Oncocytomas are usually isoechoic to the kidney, with well-demarcated margins. (Fig. 7.24) A central scar, typical of oncocytoma, may be visible with US. With CT or MR imaging, these lesions appear well circumscribed and have homogeneous enhancement patterns. Often the appearance of a pseudocapsule is seen at the periphery of the mass. The pseudocapsule is formed from renal parenchyma compressed around the edge of the mass. The above mentioned central stellate scar may also be detectable with CT (Fig. 7.25) or MR imaging. Although this scar is typical of oncocytoma, it is not diagnostic, and RCC may have an identical appearance. Angiography may be obtained prior to attempting renal-sparing surgery. The typical angiographic pattern of an oncocytoma is one of a "spoke wheel" with circumferential vessels at the periphery of the lesions and feeding vessels penetrating to the avascular central scar. These tumors lack the bizarre tumor vascularity often seen with RCC. A renal mass with these features may be an oncocytoma, but renal cell carcinoma can have identical imaging findings; thus, a renal mass with some, or all, of these features should be considered a "surgical" renal mass. At best, the presence of some of these imaging features may suggest the possibility of an oncocytoma and may prompt an attempted renal-sparing approach to the tumor. At the time of surgery, histological assessment of the entire lesion can confirm the diagnosis of oncocytoma. If malignant elements indicating an RCC are found, partial or radical nephrectomy can be completed.

Fig. 7.25. Oncocytoma in a 55-year-old man. Axial contrast-enhanced CT scan demonstrates homogenous renal mass with central stellate scar (*arrows*). Although this mass was an oncocytoma, there is considerable overlap of these imaging features with RCC.

With CT or MR imaging, MLCNs are well-defined masses with visible septations (Fig. 7.26). Internal hemorrhage is characteristically absent in these benign tumors. They are hypovascular or avascular. Like oncocytomas, these tumors have characteristic features, none of which, however, distinguish them reliably from RCC; therefore, at best, one can sug-

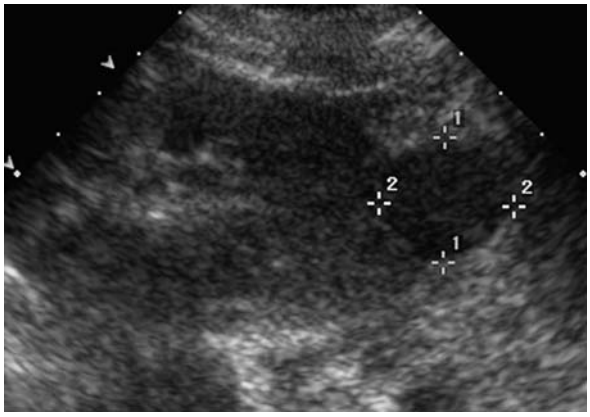

a

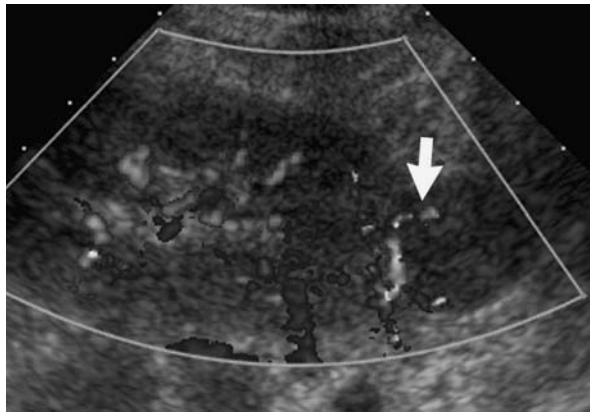

b

Fig. 7.24a,b. Oncocytoma in a 54-year-old woman. **a** Longitudinal US image shows solid lesion with homogeneous echo texture. **b** Longitudinal color Doppler image shows vessel extending from kidney into lesion (*arrow*).

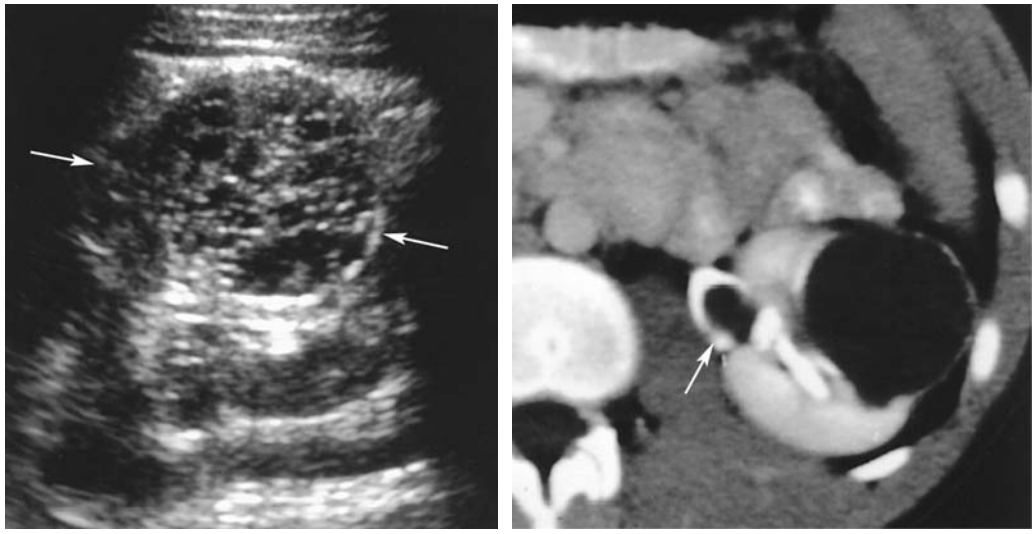

Fig. 7.26a,b. Multilocular cystic nephroma in a 42-year-old woman. **a** Oblique US image of a renal mass (*arrows*) demonstrates numerous cystic locules with interposed septa. **b** Axial contrast-enhanced CT scan of this same mass demonstrates features typical of a multilocular cystic nephroma. This cystic mass is well circumscribed with thin septations. Centrally it is seen to herniate (*arrow*) into the renal pelvis.

gest the diagnosis preoperatively, so that renal-sparing surgery can be attempted in some cases.

Tumefactive or focal XGP results from a focal area of renal inflammation often associated with stone disease. No imaging characteristics are diagnostic of focal XGP. With IVU, a hypofunctioning focal mass is evident. With US, this mass may have increased echogenicity due to the innumerable lipid-laden macrophages that make up the mass. On CT, focal XGP appears as a nonspecific solid or cystic renal mass (Fig. 7.27), often in association with a renal calculus. Typical history may suggest the diagnosis of focal XGP preoperatively. These lesions are irreversible and are best treated with renal-sparing surgery.

7.4.3 Spontaneous Perirenal Hemorrhage

Nontraumatic spontaneous renal, subcapsular, or perirenal hemorrhage (SPH; Fig. 7.28) is an unusual presentation of RCC, causing patients to seek medical evaluation. Of all SPHs, up to 55% are due to underlying RCCs (Zhang et al. 2002). Unfortunately, extensive hemorrhage often obscures the underlying tumor, making it undetectable with CT or MR imaging. In these cases, if a renal mass is not detected when SPH is initially diagnosed, a renal arteriogram should be acquired to detect evidence of a vasculitis or vascular lesion; if none is detected, CT or MR imaging should be repeated in 1 month to search again for a renal mass while the hemorrhage is resolving. Follow-up CT or MR imaging should be repeated if no lesion is detected. If a benign mass, such as an AML, which is commonly associated with SPH, is detected, it can be treated nonsurgically or with renal-sparing surgery. Detection of an RCC usually

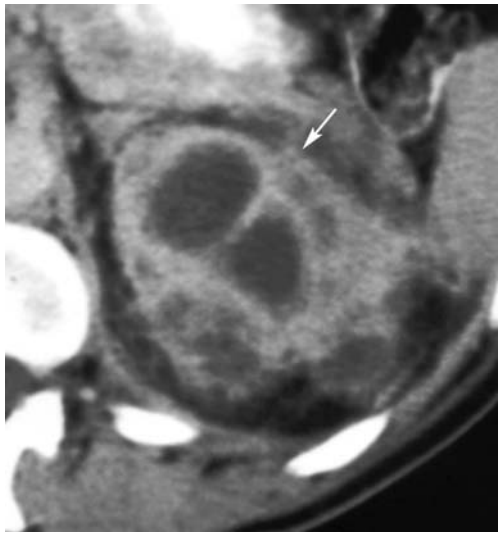

Fig. 7.27. Focal xanthogranulomatous pyelonephritis in a 50-year-old man. Axial contrast-enhanced CT scan shows multicystic ill-defined mass (*arrow*) upper pole left kidney. Renal cell carcinoma could have similar appearance.

Fig. 7.28. Spontaneous perirenal hemorrhage in a 69-year-old man with RCC. Axial unenhanced CT scan demonstrates subcapsular (*arrows*) and perirenal (*arrowheads*) hyperdense fluid. This is typical of acute hemorrhage and suggests underlying pathology in that kidney. Further scanning demonstrated a solid renal mass with features typical of RCC in this kidney.

leads to nephrectomy. This approach to SPH helps to minimize nephrectomy for benign diseases.

7.5 Conclusion

Because a significant percentage of RCCs are discovered incidentally on an imaging study ordered for another purpose, the radiologist must remain vigilant. Once a suspected mass is identified, US is a cost-effective means to further characterize those lesions that are statistically most likely to be simple cysts. Solid or complex cystic lesions are best characterized by CT or MR imaging. These cross-sectional modalities are also indispensable in the staging and restaging of suspected RCC lesions, although other modalities, such as PET, may play a complementary role.

References

American Cancer Society (1996) Cancer facts and figures – 1996. American Cancer Society, Atlanta

Bechtold RE, Zagoria RJ (1997) Imaging approach to staging of renal cell carcinoma. Urol Clin North Am 24:507–522

Bosniak MA, Birnbaum BA, Krinsky GA et al. (1995) Small renal parenchymal neoplasms: further observations on growth. Radiology 197:589–597

Bosniak MA (1997) The use of the Bosniak classification system for renal cysts and cystic tumors. J Urol 157:1852–1853

Bracken RB (1987) Renal carcinoma: clinical aspects and therapy. Semin Roentgenol 22:241–247

Chow WH, Devsa SS, Warren JL et al. (1999) Rising incidence of renal cell cancer in the United States. J Am Med Assoc 281:1628–1631

Choyke PL, Filling-Katz MR, Shawker TH et al. (1990) Von Hippel-Lindau disease: radiologic screening for visceral manifestations. Radiology 174:815–820

Eble JN, Sauter G, Epstein JI et al. (eds) (2004) Tumors of the kidney. In: WHO classification of tumours: tumours of the urinary system and male genital organs. IARC Press, Lyon, France

Einstein DM, Herts BR, Weaver R et al. (1995) Evaluation of renal masses detected by excretory urography: cost-effectiveness of sonography versus CT. Am J Roentgenol 164:371–375

Ergen FB, Hussain HK, Caoili EM (2004) MRI for preoperative staging of renal cell carcinoma using the 1997 TNM classification: comparison with surgical and pathologic staging. Am J Roentgenol 182:217–225

Fisher RI, Rosenberg SA, Fyfe G (2000) Long-term survival update for high-dose recombinant interleukin-2 in patients with renal cell carcinoma. Cancer J Sci Am 6 (Suppl 1):55–57

Forman HP, Middleton WD, Melson GL et al. (1993) Hyperechoic renal cell carcinomas: increase in detection at US. Radiology 188:431–434

Gash JR, Zagoria RJ, Dyer RB (1992) Imaging features of infiltrating renal lesions. Crit Rev Diagn Imaging 33:293–310

Greenlee RT, Murray T, Bolden S, Wingo PA (2000) Cancer statistics, 2000. CA Cancer J Clin 50:7–33

Greenlee RT, Hill-Harmon MB, Murray T, Thun M (2001) Cancer statistics, 2001. CA Cancer J Clin 51:15–36

Guinan P, Sobin LH, Algaba F (1997) TNM staging of renal cell carcinoma: Workgroup no. 3 (Union International Contre le Cancer UICC) and the American Joint Committee on Cancer (AJCC). Cancer 80:992–993

Gupta NP, Ansari MS, Khaitan A et al. (2004) Impact of imaging and thrombus level in management of renal cell carcinoma extending to veins. Urol Int 72:129–134

Ho VB, Allen SF, Hood MN et al. (2002) Renal masses: quantitative assessment of enhancement with dynamic MR imaging. Radiology 224:695–700

Jadvar H, Kherbache HM, Pinski JK et al. (2003) Diagnostic role of [F-18]-FDG positron emission tomography in restaging renal cell carcinoma. Clin Nephrol 60:395–400

Jennings CM, Gaines PA (1988) The abdominal manifestation of von Hippel-Lindau disease and a radiological screening protocol for an affected family. Clin Radiol 39:363–367

Kang DE, White RL Jr, Zuger JH et al. (2004) Clinical use of fluorodeoxyglucose F 18 positron emission tomography for detection of renal cell carcinoma. J Urol 171:1806–1809

deKernion JB (1987) Management of renal adenocarcinoma. In: deKernion JB, Paulson DF (eds) Genitourinary cancer management. Lea and Febiger, Philadelphia, pp 187–217

Kim JK, Kim TK, Ahn HJ et al. (2002) Differentiation of subtypes of renal cell carcinoma on helical CT scans. Am J Roentgenol 178:1499–1506

Landis SH, Murray T, Bolden S, Wingo PA (1998) Cancer statistics, 1998. CA Cancer J Clin 48:6–29
Landis SH, Murray T, Bolden S, Wingo PA (1999) Cancer statistics, 1999. CA Cancer J Clin 49:8–31
Leslie JA, Prihoda T, Thompson IM (2003) Serendipitous renal cell carcinoma in the post-CT era: continued evidence in improved outcomes. Urol Oncol 21:39–44
Ljungberg B (2004) Nephron-sparing-surgery strategies for partial nephrectomy in renal cell carcinoma. Scand J Surg 93:126–131
Majhail NS, Urbain J, Albani JM et al. (2003) F-18 fluorodeoxyglucose positron emission tomography in the evaluation of distant metastases from renal cell carcinoma. J Clin Oncol 21:3995–4000
Motzer RJ, Bander NH, Nanus DM (1996) Renal cell carcinoma. N Engl J Med 335:865–875
Schatz SM, Lieber MM (2003) Update on oncocytoma. Curr Urol Rep 4:30–35
Seidenwurm DJ, Barkovich AJ (1992) Understanding tuberous sclerosis. Radiology 183:23–24
Siegel SC, Sandler MA, Alpern MB et al. (1988) CT of renal cell carcinoma in patients on chronic hemodialysis. Am J Roentgenol 150:583–585
Sweeney JP, Thornhill JA, Graiger R et al. (1996) Incidentally detected renal cell carcinoma: pathological features, survival trends and implications for treatment. Br J Urol 78:351
Takahashi K, Honda M, Okubo RS et al. (1993) CT pixel mapping in the diagnosis of small angiomyolipomas of the kidneys. J Comput Assist Tomogr 17:98–101
Watson RC, Fleming RJ, Evans JA (1968) Arteriography in the diagnosis of renal carcinoma: review of 100 cases. Radiology 91:888–897
Welch TJ, LeRoy AJ (1997) Helical and electron beam CT scanning in the evaluation of renal vein involvement in patients with renal cell carcinoma. J Comput Assist Tomogr 21:467–471
Yagoda A, Abi-Rached B, Petrylak D (1995) Chemotherapy for advanced renal-cell carcinoma: 1983–1993. Semin Oncol 22:42–60
Yamashita Y, Ueno S, Makita O et al. (1993) Hyperechoic renal tumors: anechoic rim and intratumoral cysts in US differentiation of renal cell carcinoma from angiomyolipoma. Radiology 188:179–182
Zagoria RJ, Wolfman NT, Karstaedt N et al. (1990) CT features of renal cell carcinoma with emphasis on relation to tumor size. Invest Radiol 25:261–266
Zhang JQ, Fielding JR, Zou KH (2002) Etiology of spontaneous perirenal hemorrhage: a meta-analysis. J Urol 167:1593–1596